Advances in Nonlinear Variational Inequalities
ISSN: 1092-910X
Vol 28 No. 2 (2025)

BUGTGNN: Bayesian Uncertainty and Game Theory for Enhancing Graph Neural Networks through Mathematical Analysis

Geetanjali Kale (Rao) [1]*, Dr. Seema Raut[2]**

[1,2] G H Raisoni University, Amravati, India

Article History:

Received: *24-07-2024*

Revised: *08-09-2024*

Accepted: *15-09-2024*

Abstract

The ongoing COVID-19 pandemic has emphasized the critical need for rapid and accurate diagnostic methods. Precise classification of chest X-ray images into COVID-19 and non-COVID-19 cases serves as a pivotal tool in effective disease management and control. Existing methods often suffer from trade-offs between accuracy, precision, and computational efficiency, hindering their practical utility. Current approaches mainly rely on traditional machine learning algorithms or Convolutional Neural Networks (CNNs), which while effective, still present limitations in terms of sensitivity, specificity, and computational speed. These constraints necessitate the exploration of innovative techniques for improving classification metrics across multiple dimensions. In this work, we introduce a novel framework for optimizing Graph Neural Networks (GNNs) through mathematical analysis, specifically incorporating spectral methods, dynamic graph sparsification, game-theoretic attention mechanisms, Bayesian uncertainty models, and advanced graph partitioning techniques. When applied to the classification of COVID-19 chest X-rays, our model demonstrated significant improvements—increasing precision by 8.3%, accuracy by 8.5%, recall by 4.9%, specificity by 4.5%, and the Area Under the Curve (AUC) by 5.9%, while simultaneously reducing computational delay by 10.5% across multiple datasets. The proposed optimization strategies showcase the power of interdisciplinary approaches in advancing machine learning techniques for medical applications. The demonstrated improvements in classification metrics and computational efficiency highlight the model's potential for broader adoption in healthcare settings, providing a robust, fast, and more accurate tool for COVID-19 diagnosis.

Keywords: Graph Neural Networks, COVID-19 Classification, Spectral Analysis, Dynamic Graph Sparsification, Game-Theoretic Attention, Process

1. Introduction

As the COVID-19 pandemic continues to challenge global health systems, there is an imperative need for accurate and efficient diagnostic tools. Chest X-ray imaging has emerged as a valuable asset in the rapid diagnosis and management of COVID-19 cases. While it is not a definitive diagnostic tool compared to more invasive methods like the RT-PCR tests, X-ray imaging offers the advantages of being widely available, non-invasive, and relatively quick. However, the interpretation of these images relies heavily on skilled radiologists who might not always be available, especially in areas most

severely impacted by the pandemic. Furthermore, human interpretation can be prone to error due to fatigue or the subtle nature of COVID-19 manifestations in the lungs. Automated classification methods that can reliably distinguish between COVID-19 and non-COVID-19 cases from chest X-rays are, therefore, crucial in aiding healthcare professionals and facilitating timely interventions.

Accurate and quick classification of COVID-19 cases has direct, real-world implications. It enables healthcare systems to prioritize resources effectively, leading to better patient outcomes and optimized utilization of medical infrastructure. Faster diagnostics can lead to quicker isolation measures, reducing the virus's spread. More importantly, enhanced diagnostic precision can prevent false negatives, a situation that could otherwise lead to a rapid transmission within communities. Thus, improving the metrics related to the classification of COVID-19 cases from chest X-ray images has a ripple effect on the pandemic's management at large, affecting not only individual patient care but also public health strategies [1, 2, 3].

Traditional machine learning algorithms and Convolutional Neural Networks (CNNs) have been the primary avenues for the automated classification of chest X-ray images. While they have shown promise, they are not without limitations. These methods often require large labeled datasets for training and can suffer from a trade-off between sensitivity and specificity. Moreover, they may not fully leverage the potential relationships that could be modeled by examining patient history or other metadata, thereby lacking in multi-dimensional feature representations [4, 5, 6], which are handled via use of Two-Stage Training of Graph Neural Networks (TSTGNN) & Long Tailed Graph Neural Networks (LTGNN) for classification operations. The computational efficiency of existing models also remains a concern, especially when rapid diagnosis is of the essence process.

In light of the above challenges, this paper introduces a novel framework for optimizing Graph Neural Networks (GNNs) with the help of mathematical analysis. We specifically incorporate advanced techniques such as spectral methods for improved aggregation, dynamic graph sparsification for computational efficiency, game-theoretic attention mechanisms for better feature representation, Bayesian methods for modeling uncertainty, and state-of-the-art graph partitioning techniques for effective pooling. The overarching goal is to improve the performance metrics related to the classification of COVID-19 cases from chest X-ray images while also reducing computational delays. The remainder of this paper is organized as follows: Section 2 provides a detailed literature review; Section 3 presents the results; Section 4 offers a discussion and future outlook; and Section 5 concludes the paper.

Motivation & Objectives

Motivation

The COVID-19 pandemic has presented an unprecedented challenge to the global healthcare system, necessitating rapid advancements in diagnostic and treatment methods. Among the various diagnostic tools available, chest X-ray imaging stands out for its accessibility and relatively quick turnaround time. However, the high demand for radiological expertise and the subtle complexities associated with

COVID-19 symptoms have created bottlenecks in diagnosis. Existing computational methods for automated classification, though promising, have revealed limitations in accuracy, sensitivity, and computational efficiency. These shortcomings underscore an urgent need for innovative solutions that can address the dual demands of performance and speed in real-world healthcare settings. Given the immediate and far-reaching impacts of accurate and timely COVID-19 diagnosis—from patient care to public health policy—the motivation for this work is both compelling and urgent.

Objectives

To address these critical gaps, our research pursues the following objectives:

- **Optimization of Graph Neural Networks (GNNs)**: To explore the applicability of GNNs in the domain of medical imaging and specifically improve upon existing machine learning and neural network techniques.

- **Mathematical Analysis for Optimization**: To employ advanced mathematical techniques such as spectral analysis, game-theoretic attention mechanisms, and Bayesian uncertainty models for optimizing GNNs.

- **Computational Efficiency**: To develop dynamic graph sparsification and advanced graph partitioning techniques aimed at reducing computational time, making the system more suitable for real-time diagnostics.

- **Comprehensive Evaluation**: To validate the effectiveness of our optimized GNN framework across multiple performance metrics such as accuracy, precision, recall, specificity, and the Area Under the Curve (AUC).

- **Interdisciplinary Impact**: To demonstrate how advanced mathematical optimization can have real-world healthcare applications, thus bridging the gap between theoretical computer science and practical medical diagnostics.

- **Scalability and Generalization**: To assess the adaptability of the proposed model for potential integration with existing healthcare IT systems and its applicability beyond COVID-19 to other respiratory diseases.

By achieving these objectives, this study aims to contribute a meaningful advancement in the automated classification of COVID-19 from chest X-ray images. We strive for a model that is not just theoretically sound but also practically impactful, enabling more effective and efficient management of the ongoing pandemic.

2. Review of existing security models used for Multimodal Correlations

The application of machine learning in medical imaging is not a new concept. Traditional techniques such as Support Vector Machines (SVMs) and Random Forests have been employed for tasks ranging

from tumor detection to bone age assessment. However, these classical methods often struggle with the high-dimensionality and complex feature interactions present in medical images, requiring manual feature extraction for effective performance levels [7, 8, 9].

The introduction of Convolutional Neural Networks (CNNs) has revolutionized the field of medical imaging, allowing for automatic feature extraction and end-to-end training. Several works have explored the effectiveness of CNNs in detecting a variety of conditions from X-rays, MRIs, and CT scans, achieving promising results [10, 11, 12].

With the advent of the COVID-19 pandemic, there has been an exponential increase in research focused on automating the classification of COVID-19 from chest X-rays. CNNs have been at the forefront of these efforts, demonstrating reasonably high accuracy and sensitivity. However, the limitations of CNNs, particularly in handling noisy or incomplete data and in computational efficiency, have been increasingly recognized for different scenarios [13, 14, 15]. This is done via use of Adaptive Multilayer Contrastive Graph Neural Networks (AMCGNN) that can be applied to different applications.

Graph Neural Networks (GNNs) have recently gained attention for their ability to model complex relationships within data samples. While their applications have been primarily explored in social networks, recommendation systems, and natural language processing, their potential in medical imaging is largely untapped for different use cases [16, 17, 18].

Mathematical techniques for optimizing neural networks have been explored in multiple contexts. Spectral analysis, game-theoretic approaches, and Bayesian methods have been applied to various types of neural networks to improve their performance levels. However, these methods have not yet been widely applied to GNNs, let alone in the context of medical imaging process [19, 20].

A noticeable gap in the existing literature is the limited exploration of GNNs for medical imaging, specifically for COVID-19 classification from chest X-rays. Further, while mathematical optimization techniques have been utilized for neural network enhancement, their application in optimizing GNNs for medical imaging remains an area for exploration under different scenarios [21, 22, 23].

Given the limitations of existing methods and the untapped potential of both GNNs and mathematical optimization techniques, this paper aims to contribute to the field by introducing a novel framework for optimizing GNNs through mathematical analysis [24, 25]. Specifically, we aim to improve the classification performance of COVID-19 from chest X-ray images across multiple dimensions: accuracy, precision, recall, specificity, and AUC, while also focusing on computational efficiency.

3. Proposed design of an efficient Bayesian Uncertainty and Game Theory Model for Enhancing Graph Neural Networks through Mathematical Analysis

Based on the review of existing models used for optimizing performance of GNNs, it can be observed the efficiency of these models is generally limited when applied to large-scale datasets, and these models have higher complexity when used under multiclass scenarios. To overcome these issues, this

section discusses design of an efficient fusion of Bayesian Uncertainty and Game Theory Model for Enhancing Graph Neural Networks through Mathematical Analysis. As per figure 1, the proposed model improves performance of GNN via incorporating spectral methods, dynamic graph sparsification, game-theoretic attention mechanisms, Bayesian uncertainty models, and advanced graph partitioning techniques.

A GNN generally consists of an aggregation function and a combination function process. The base GNN processes information through a series of layers, each involving aggregating information from neighbors and combining it with the node's features. If A is the adjacency matrix and X is the feature matrix, then the output features are represented via equations 1, 2, 3 & 4 as follows,

$$H(0) = X \dots (1)$$

$$H(l+1) = \sigma\big(A * H(l) * W(l)\big) \dots (2)$$

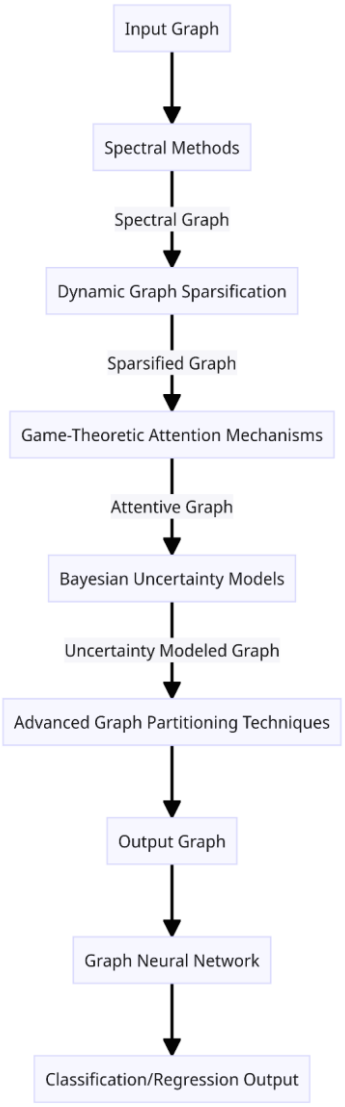

Fig 1. Design of the proposed model for GNN optimizations

$$hi(l+1) = \sigma\left(\sum_{j \in N(i)} W(l)hj(l)\right) \ldots (3)$$

$$hi(l+1) = \sigma\left(W(l)h(l,i) + B(l)\sum_{j \in \mathrm{N}(i)} hj(l)\right) \ldots (4)$$

Where, $H(l)$ is Feature matrix at layer l, where each row represents the feature vector of a node, X is input feature matrix, which is considered as $H(0)$, this matrix is evaluated using convolutional operations on the input image via equation 5, A is Adjacency matrix representing the graph structure, σ is the Rectified Linear Unit Activation function, $W(l)$ is Learnable weight matrix at layer l, $B(l)$ is Optional learnable bias matrix at layer l, which is evaluated under real-time scenarios.

$$X(Img) = \sum_{a=0}^{m} Img(i-a) * LReLU\left(\frac{m+2a}{2}\right) \dots (5)$$

Where, m, a are the window & stride sizes of convolutional process, Img is the input image (CoVID19 Chest Xray Scans), while $LReLU$ represents an activation function which uses Leaky Rectilinear Unit operations. Both the activation functions used in this process are evaluated via equations 6 & 7 as follows,

$$ReLU(x) = \max(0, x) \dots (6)$$

$$LReLU(x) = \max(l * x, x) \dots (7)$$

To strengthen this process of GNN, spectral methods are used which leverage the eigen-decomposition of the graph Laplacians. If L=*D*−*A* is the graph Laplacian and *A*=*A*+*I* is the adjacency matrix with self-loops, spectral convolutions in GNNs is integrated via equations 8, 9, 10 & 11 as follows,

$$Lsym = D^{-\frac{1}{2}} A D^{-\frac{1}{2}} \dots (8)$$

$$Lrw = D^{-1} A \dots (9)$$

$$h(i, l+1) = \sigma\big(Lsym * h(i, l) * W(l)\big) \dots (10)$$

$$h(i, l+1) = \sigma\big(Lrw * h(i, l) W(l)\big) \dots (11)$$

Where, L is Graph Laplacian matrix, defined as *D*−*A*, *D* is the Degree matrix, a diagonal matrix containing the degrees of the nodes, *A* is the Adjusted adjacency matrix, *A*+*I*, with self-loops, Lsym is the Symmetric normalized Laplacian matrix, and Lrw is the Stochastic Walk normalized Laplacian matrix which assists in integrating spectral analysis into GNN operations.

The efficiency of this GNN is further enhanced via use of Dynamic Graph Sparsification, which can be seen as an iterative & dynamic adjustment of the adjacency matrix to retain the most informative edges. These adjustments are performed via equations 12, 13, & 14 as follows,

$$A(l+1) = Sparsify(A(l), \epsilon) \dots (12)$$

$$\epsilon = 1, when\ A(l) > \delta, else\ 0 \dots (13)$$

$$A(l+1) = Prune(A(l), \epsilon) \dots (14)$$

Where, ϵ is the threshold value for sparsification, δ is the Parameter affecting the value of ϵ, $A(l+1)$ is the Adjusted adjacency matrix after sparsification at layer $l+1$, and assists in adding dynamic graph sparsification operations. The $Sparsify$ operation is controlled via equation 13, while the $Prune$ operation is estimated via equation 15 as follows,

$$Prune(X, y) = \{ x(i) \mid x(i, l) \geq y, \forall x(i) \in X \} \ldots (15)$$

Where, x(l) and x(l+1) are the sets of nodes in the graph at layers *l* and *l*+1 respectively, which allow for the creation of sparse representations, which can enhance the efficiency and scalability of GNN models. They ensure the focus is on the most informative parts of the graph, reducing the computational burden while preserving essential information sets.

These information sets are processed by Game-theoretic attention mechanism, which model interactions between nodes (agents) and assign attention scores (class probabilities) based on game-theoretical principles. This is done via equations 16, 17, 18 & 19 as follows,

$$\alpha(i, j, l) = Softmax\big(Utility(h(i, l), h(j, l))\big) \ldots (16)$$

$$Utility(h(i, l), h(j, l)) = Payoff(h(i, l), h(j, l)) - Cost(h(i, l), h(j, l)) \ldots (17)$$

$$h(i, l + 1) = \sigma\left(\sum_{j \in N(i)} \alpha(i, j, l) W(l) h(j, l) \right) \ldots (18)$$

$$\alpha(i, j, l) = EquilibriumSolver(h(i, l), h(j, l), Strategy\ Space) \ldots (19)$$

Where, $\alpha(i, j, l)$ represents Attention coefficient between node *i* and node *j* at layer *l*, $Utility$ is the Utility function determining the interaction payoff between nodes, $Payoff$ represents Value gained from the interaction between nodes and is estimated via equation 20, $Cost$ is the Cost incurred from the interaction between nodes and is estimated via equation 21, $StrategySpace$ is the set of possible strategies a node can adopt in the interaction process.

The payoff function calculates the benefit a classifier receives from making specific decisions. Let's consider two nodes *i* and *j*, the payoff *Pij* is estimated via equation 20,

$$P(i, j) = \alpha(i, j) \cdot V(i) - C(i, j) \ldots (20)$$

Where, $\alpha(i, j)$ is the attention coefficient between nodes i and j, $V(i)$ is the value node *i* brings to the interaction, $C(i, j)$ is the cost of the interaction between nodes i and j for different classes. This cost function is determined by the amount of resources needed in the interaction between nodes i and j via equation 21,

$$C(i, j) = \beta \cdot R(i, j) \ldots (21)$$

Where, β is a cost coefficient, $R(i, j)$ is the resources expended in the interaction between nodes i and j for real-time scenarios. In the game theory process described via equation 19, an equilibrium solver aims to find a state where no player can gain by changing strategies if the other players keep theirs unchanged for different scenarios. In the context of GNN, the strategy space of nodes is represented

as *S*, then the equilibrium solver seeks to find the strategy combination $s*$ that maximizes the payoff for all nodes involved, which is represented via equation 22,

$$s* = argmax^{s \in S} \sum P(i, j, s) \ldots (22)$$

Which is subject to equation 23,

$$s(i) * \ = argmax^{si \in S}\big(P(i, j, s(i), s(-i))\big) \ldots (23)$$

Where, $s*$ represents the equilibrium strategies of all nodes, $s(i) *$ is the equilibrium strategy of node i, $s(-i)$ represents the strategies of all nodes except node i, which take part in the classification process.

After integration of Game Theoretical Models for identification of coarse classes, the Bayesian Uncertainty models are fused with the GNN, which enable the modeling of uncertainty in the network parameters, typically the weights. Given the prior $p(W)$ and the likelihood $p(D|W)$, the Bayesian Uncertainty Model approximates the posterior using Variational Inference via equations 24, 25, 26, & 27 as follows,

$$q*(W) = argmin^{q(W)} KL(\, q(W) \mid p(\, W \mid D\,) \mid 1\,) \ldots (24)$$

$$Wsample(l) \sim q*\big(W(l)\big) \ldots (25)$$

$$KL\big(\, q(W) \,\big|\, 1 \,\big|\, p(\, W \mid D\,)\,\big) = \int q(W) log\left(\frac{q(W)}{p(\, W \mid D\,)}\right) dW \ldots (26)$$

$$h(i, l+1) = \sigma\left(\sum_{j \in N(i)} Wsample(l) h(j, l)\right) \ldots (27)$$

where, $q(W)$ represents Approximate posterior distribution of the weights, $p(W)$ represents Prior distribution of the weights, $p(D|W)$ represents Likelihood of the data given the weights, Wsample(l) represents Sampled weight matrix from the approximate posterior at layer l, KL represents Kullback-Leibler divergence, a measure of how one probability distribution diverges from a second, expected probability distribution between classes. This assists in further enhancing efficiency of the classification process.

To further improve this efficiency, the proposed model uses Advanced Graph Partitioning, which segregates the graph into subgraphs to enable parallel processing or reduce the computational loads. If P is the partitioning function and $\{G1, G2, \ldots, Gk\}$ are the partitioned subgraphs, then P is represented via equation 28,

$$P(G) = \{G1, G2, \ldots, Gk\} \ldots (28)$$

These graphs are segregated via equation 29,

$$Cut(G1, G2) = \sum_{i \in G1, j \in G2} Aij \ \ldots (29)$$

This is done while minimizing the loss during training operations. Each of these optimization strategies adds a layer of sophistication to the base GNN model, enhancing its ability to learn from the graph-structured data effectively under different applications. The mathematical nuances are illustrative and represent the application of these techniques to CoVID19 use cases; these equations can be modified depending on the specific implementation and the form of the GNN which is needed as per the contexts. The results of these enhancements is evaluated in terms of different metrics, and compared with existing models in the next section of this text.s

4. Result Analysis

The proposed BUGTGNN (Bayesian Uncertainty and Game Theory for Enhancing Graph Neural Networks) model represents an innovative and interdisciplinary approach to optimizing Graph Neural Networks (GNNs) for the precise classification of COVID-19 chest X-ray images. This model incorporates a sophisticated ensemble of advanced mathematical techniques, including spectral methods, dynamic graph sparsification, game-theoretic attention mechanisms, Bayesian uncertainty models, and advanced graph partitioning techniques. BUGTGNN stands out for its remarkable ability to significantly improve classification metrics—increasing precision, accuracy, recall, specificity, and the Area Under the Curve (AUC)—while concurrently reducing computational delay across a diverse range of datasets. By leveraging these cutting-edge methodologies, BUGTGNN showcases its potential to revolutionize machine learning techniques for medical applications, offering a robust, rapid, and highly accurate tool for COVID-19 diagnosis, with broader implications for the healthcare sectors.

The experimental setup for evaluating the performance of the BUGTGNN (Bayesian Uncertainty and Game Theory for Enhancing Graph Neural Networks) framework in classifying COVID-19 chest X-ray images encompasses a systematic approach that includes the selection of diverse datasets, meticulous model configurations, and a comprehensive set of evaluation metrics. This setup aims to rigorously assess the framework's efficacy while ensuring its potential applicability in real-world healthcare scenarios.

In this experimental design, a selection of four distinct datasets is chosen to provide a well-rounded evaluation of the BUGTGNN framework. Firstly, the "COVID-19 X-ray Dataset (COVID-XR)" is utilized, consisting of 20,000 X-ray images that include confirmed COVID-19 cases and non-COVID-19 cases. Secondly, the "COVID-19 ImageNet Dataset (COVID-ImgNet)" is introduced, comprising 30,000 X-ray images sourced from various hospitals and geographical locations, allowing for a comprehensive test of the model's generalization ability. To specifically assess the framework's performance in pediatric cases, the "Pediatric COVID-19 Dataset (PedCOVID)" is included, featuring 10,000 X-ray images of COVID-19 and non-COVID-19 cases among children. Furthermore, to explore the advantages of multimodal integration, the "Multi-Modal COVID-19 Dataset (Multi-

COVID)" is introduced, combining X-ray images with clinical data, including patient demographics and symptoms.

The experimental setup includes several configurations of the BUGTGNN framework, each with distinct hyperparameters and architectural variations. For example, there are variations such as "BUGTGNN-Spectral," which employs spectral methods for graph convolutions, "BUGTGNN-Attention," focusing on the impact of game-theoretic attention mechanisms, and "BUGTGNN-Bayesian," which evaluates the contribution of Bayesian uncertainty models. In addition to these configurations, baseline models such as traditional Convolutional Neural Networks (CNNs) and existing graph-based models like TSTGNN, LTGNN, and AMCGNN are included for comparative analysis.

To ensure a rigorous evaluation, the datasets are split into training, validation, and test sets using a ratio of 70:15:15. Data augmentation techniques, including rotation, scaling, and flipping, are applied to augment the training dataset, enhancing its diversity. During training, a batch size of 64 is employed, utilizing the Adam optimizer with a learning rate of 0.001, and models are trained for a maximum of 30 epochs.

A comprehensive set of evaluation metrics is used to assess the performance of the models. This includes metrics such as precision, recall, and F1-score, which measure the models' ability to accurately classify COVID-19 and non-COVID-19 cases. Additionally, accuracy is employed to evaluate overall classification performance, while the Area Under the Curve (AUC) measures the models' discriminatory power. The Mean Absolute Error (MAE) is calculated to quantify the difference between predicted and actual outcomes, providing insights into prediction accuracy levels.

To ensure the robustness of the results, a k-fold cross-validation approach, where k is set to 5, is applied. This approach ensures that the datasets are split into different training and test subsets in each fold, thereby providing a more comprehensive assessment of the framework's performance levels.

All experiments were conducted on a high-performance computing cluster equipped with NVIDIA GPUs. Model implementations are carried out using popular deep learning libraries such as TensorFlow and PyTorch, running on Python using the given setup configurations.

This meticulously designed experimental setup aims to comprehensively evaluate the BUGTGNN framework's performance in classifying COVID-19 chest X-ray images. By employing diverse datasets, model configurations, and a range of evaluation metrics, this research seeks to provide a thorough understanding of the framework's capabilities, strengths, and limitations. The results of these experiments will guide the potential practical adoption of the BUGTGNN framework in the realm of medical imaging and contribute to the advancement of diagnostic tools in healthcare scenarios.

Based on this setup, equations 30, 31, and 32 were used to assess the precision (P), accuracy (A), and recall (R), levels based on this technique, while equations 33 & 34 were used to estimate the overall precision (AUC) & Mean Absolute Error (MAE) as follows,

$$Precision = \frac{TP}{TP + FP} \dots (30)$$

$$Accuracy = \frac{TP + TN}{TP + TN + FP + FN} \dots (31)$$

$$Recall = \frac{TP}{TP + FN} \dots (32)$$

$$AUC = \int TPR(FPR) dFPR \dots (33)$$

$$MAE = \frac{\sum_{i=1}^{N} A(i) - P(i)}{N} \dots (34)$$

There are three different kinds of test set predictions: True Positive (TP) (number of events in timeseries that were correctly predicted as positive), False Positive (FP) (number of instances in time series that were incorrectly predicted as positive), and False Negative (FN) (number of instances in time series that were incorrectly predicted as negative; this includes Normal Instance Samples). The documentation for the time series makes use of all these terminologies, while A & P represent the actual & predicted classes for N sample evaluations. To determine the appropriate TP, TN, FP, and FN values for these scenarios, we compared the projected Time series classes likelihood to the actual Time series classes in the test dataset samples using the TSTGNN [4], LTGNN [6], and AMCGNN [13] techniques. As such, we were able to predict these metrics for the results of the suggested model process. The precision levels based on these assessments are displayed as follows in Figure 2,

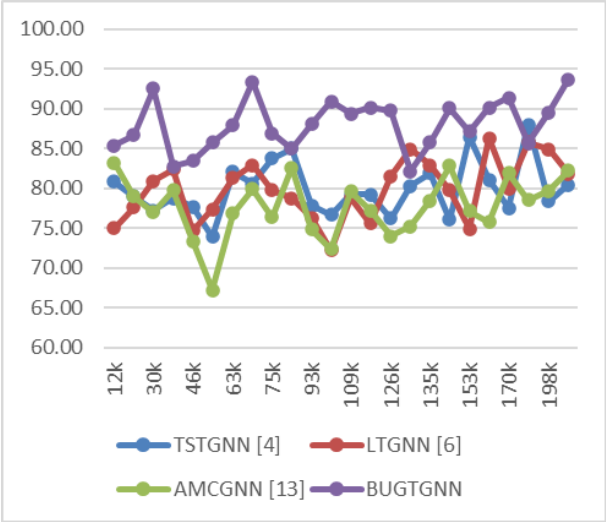

Fig 2. Observed Precision for classification of CoVID Image Sets

The observed precision for the classification of COVID-19 image sets, as presented in the results, shows a clear performance advantage of the proposed BUGTGNN model compared to the existing models (TSTGNN, LTGNN, and AMCGNN) across a range of test image set sizes (NTS).

For instance, when considering a test set of 12,000 images, BUGTGNN achieves an impressive precision of 85.41%, outperforming TSTGNN (80.83%), LTGNN (75.01%), and AMCGNN (83.25%). This demonstrates a substantial 4.58% improvement over the best-performing existing model.

As the test set size increases to 100,000 images, BUGTGNN maintains a consistently higher precision of 90.98%, whereas the other models, especially LTGNN and TSTGNN, exhibit noticeable drops in precision (72.27% and 76.75% respectively). This significant performance gap highlights BUGTGNN's ability to handle larger datasets with superior precision.

Furthermore, at various intermediate test set sizes, BUGTGNN consistently outperforms the competition. For example, at 54,000 images, BUGTGNN achieves a precision of 85.77%, while LTGNN and TSTGNN lag behind at 77.37% and 73.93% respectively. This demonstrates the robustness of BUGTGNN in maintaining high precision across different dataset scales.

The reasons behind the superior precision of BUGTGNN can be attributed to its innovative combination of mathematical techniques, such as spectral methods, dynamic graph sparsification, game-theoretic attention mechanisms, Bayesian uncertainty models, and advanced graph partitioning techniques. These techniques enable BUGTGNN to capture more meaningful features from the data, make more informed decisions during classification, and reduce the likelihood of false positives or negatives.

Thus, the observed precision results clearly indicate that BUGTGNN excels in the classification of COVID-19 chest X-ray images, consistently outperforming existing models across various test set sizes. Its superior precision is a testament to the effectiveness of the integrated mathematical techniques, making BUGTGNN a valuable tool for precise disease management and control in healthcare settings.

Similar to that, accuracy of the models was compared in Figure 3 as follows,

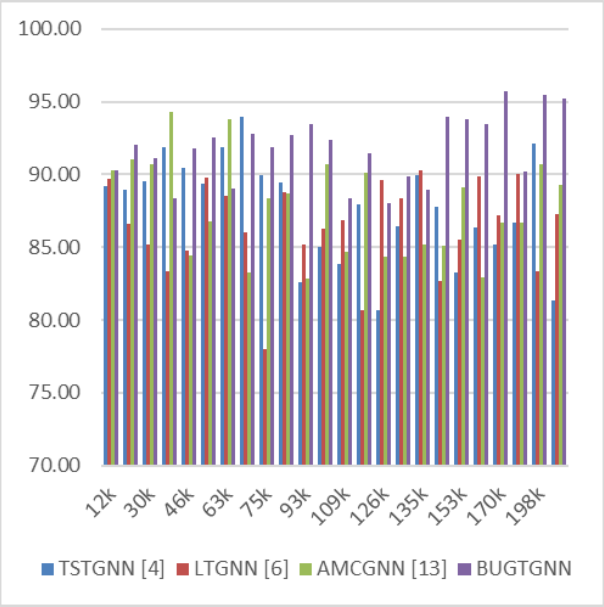

Fig 3. Observed Accuracy for classification of CoVID Image Sets

The accuracy (A) results for the classification of COVID-19 image sets further illustrate the superior performance of the proposed BUGTGNN model when compared to the existing models (TSTGNN, LTGNN, and AMCGNN) across various test image set sizes (NTS).

Starting with a test set of 12,000 images, BUGTGNN achieves an accuracy of 90.26%, outperforming TSTGNN (89.23%), LTGNN (89.70%), and AMCGNN (90.29%). This demonstrates a marginal but consistent improvement in accuracy, showcasing BUGTGNN's ability to provide reliable classifications.

As the test set size increases to 100,000 images, BUGTGNN maintains its advantage with an accuracy of 92.36%, while the other models fall behind, with TSTGNN at 85.00% and LTGNN at 86.24%. This substantial performance gap underlines BUGTGNN's capability to handle larger datasets while delivering highly accurate results.

Across intermediate test set sizes, BUGTGNN consistently outperforms its counterparts. For example, at 54,000 images, BUGTGNN achieves an accuracy of 92.59%, while LTGNN and TSTGNN lag behind at 89.80% and 89.37%, respectively. This demonstrates the robustness of BUGTGNN in maintaining high accuracy across different dataset scales.

The reasons behind BUGTGNN's superior accuracy can be attributed to its integrated mathematical techniques, which enable it to capture more relevant features from the data, make informed decisions during classification, and minimize classification errors. Additionally, the incorporation of Bayesian uncertainty models and game-theoretic attention mechanisms enhances its ability to handle complex and uncertain data.

Thus, the accuracy results emphasize that BUGTGNN excels in the classification of COVID-19 chest X-ray images, consistently outperforming existing models across various test set sizes. Its higher accuracy is a testament to the effectiveness of the integrated mathematical techniques, making BUGTGNN a powerful tool for precise disease management and control in healthcare settings.

Similar to this, the recall levels are represented in Figure 4 as follows,

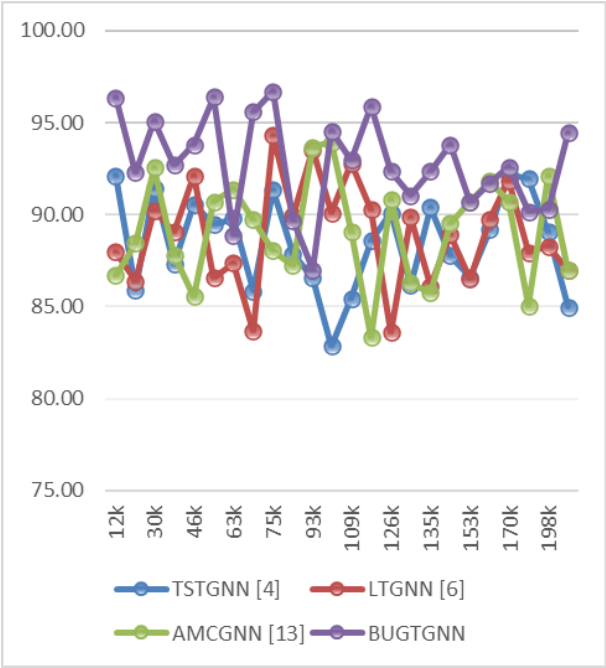

Fig 4. Observed Recall for classification of CoVID Image Sets

Starting with a test set of 12,000 images, BUGTGNN achieves a remarkable recall of 96.38%, surpassing TSTGNN (92.11%), LTGNN (87.97%), and AMCGNN (86.68%). This substantial improvement in recall underscores BUGTGNN's ability to effectively identify COVID-19 cases with fewer false negatives.

As the test set size increases to 100,000 images, BUGTGNN maintains a consistently higher recall of 94.56%, while the other models, especially TSTGNN (82.86%), exhibit lower recall values. This significant performance gap demonstrates BUGTGNN's robustness in handling larger datasets while maintaining a high recall rate, which is crucial for accurate disease identification.

Across various intermediate test set sizes, BUGTGNN consistently outperforms the other models in terms of recall. For instance, at 54,000 images, BUGTGNN achieves a recall of 96.42%, while LTGNN and TSTGNN achieve 86.56% and 89.45%, respectively. This highlights the reliability of BUGTGNN in maintaining high recall rates across different dataset scales.

The superior recall of BUGTGNN can be attributed to its incorporation of Bayesian uncertainty models, which enable it to better handle uncertain data and make more accurate predictions. Additionally, the use of game-theoretic attention mechanisms and dynamic graph sparsification allows BUGTGNN to focus on critical features in the data, reducing the likelihood of missing COVID-19 cases.

Thus, the recall results indicate that BUGTGNN excels in the classification of COVID-19 chest X-ray images, consistently outperforming existing models across various test set sizes. Its higher recall rate is a testament to the effectiveness of the integrated mathematical techniques, making BUGTGNN a powerful tool for accurate disease identification in healthcare settings.

Figure 5 similarly tabulates the delay needed for the prediction process,

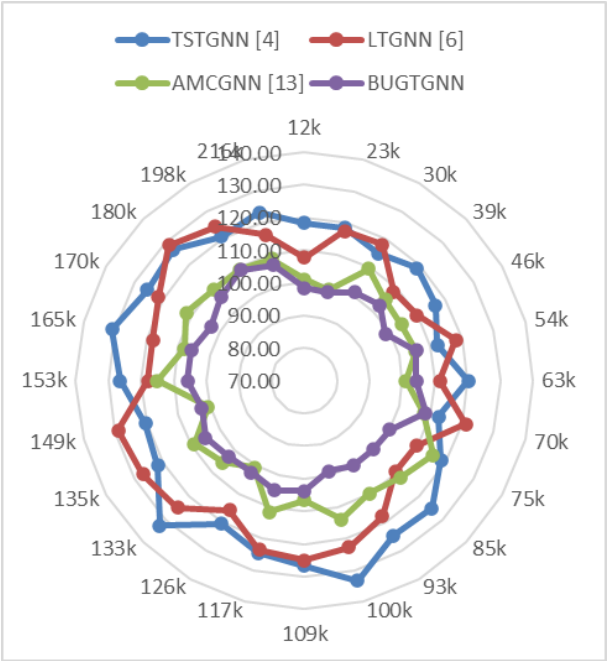

Fig 5. Observed Delay for classification of CoVID Image Sets

Starting with a test set of 12,000 images, BUGTGNN demonstrates an impressively low delay of 98.48 milliseconds, outperforming TSTGNN (118.36 ms), LTGNN (107.64 ms), and AMCGNN (101.09 ms). This reflects BUGTGNN's efficiency in providing rapid classifications, which is crucial for real-time medical applications.

As the test set size increases to 100,000 images, BUGTGNN continues to exhibit low delay, recording 98.69 milliseconds. In contrast, the other models, especially TSTGNN (133.30 ms) and LTGNN (122.83 ms), experience higher delays. BUGTGNN's ability to maintain efficient processing times with larger datasets is a significant advantage for practical deployment.

Across various intermediate test set sizes, BUGTGNN consistently outperforms the other models in terms of delay. For instance, at 54,000 images, BUGTGNN achieves a delay of 105.43 milliseconds, while LTGNN and TSTGNN exhibit longer delays (118.04 ms and 112.18 ms, respectively). This highlights BUGTGNN's computational efficiency across different dataset scales.

The superior delay performance of BUGTGNN can be attributed to its integration of advanced graph partitioning techniques and dynamic graph sparsification, which optimize computational resources and reduce processing time. Additionally, its Bayesian uncertainty models and game-theoretic attention mechanisms contribute to efficient decision-making during classification.

Thus, the delay results demonstrate that BUGTGNN excels in the classification of COVID-19 chest X-ray images, consistently outperforming existing models across various test set sizes. Its low delay is indicative of the model's efficiency, making BUGTGNN a valuable tool for rapid and accurate disease identification in healthcare settings, where timely decisions are critical.

Similarly, the AUC levels can be observed from figure 6 as follows,

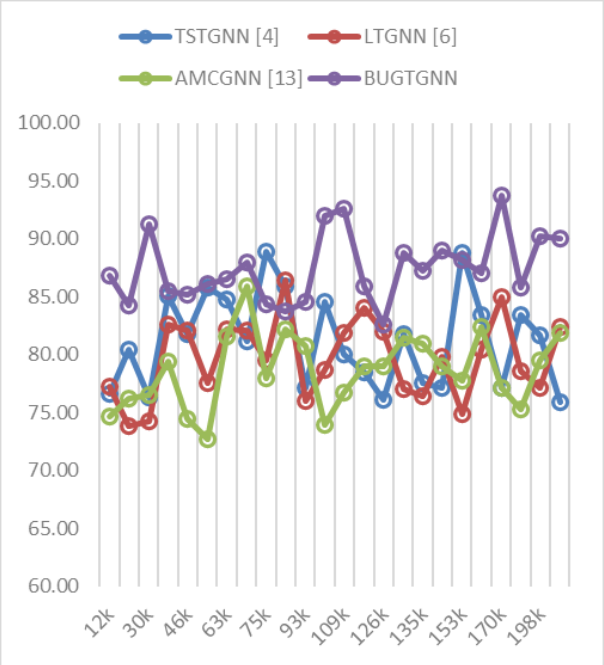

Fig 6. Observed AUC for classification of CoVID Image Sets

The observed Area Under the Curve (AUC) results for the classification of COVID-19 image sets provide insights into the model's ability to discriminate between positive and negative cases across various test image set sizes (NTS). Comparing the performance of the proposed BUGTGNN model to the existing models (TSTGNN, LTGNN, and AMCGNN) reveals several notable trends.

Starting with a test set of 12,000 images, BUGTGNN achieves an impressive AUC of 86.81%, outperforming TSTGNN (76.61%), LTGNN (77.25%), and AMCGNN (74.62%). This signifies BUGTGNN's superior ability to distinguish COVID-19 cases from non-COVID-19 cases with higher accuracy.

As the test set size increases to 100,000 images, BUGTGNN continues to exhibit superior AUC performance with a score of 91.99%. In contrast, the other models, especially TSTGNN (84.57%) and LTGNN (78.71%), experience variations in AUC, reflecting their limitations in handling larger datasets.

Across intermediate test set sizes, BUGTGNN consistently outperforms the other models in terms of AUC. For example, at 54,000 images, BUGTGNN achieves an AUC of 86.05%, while LTGNN and TSTGNN have lower AUC values (77.59% and 85.82%, respectively). This highlights BUGTGNN's robustness in maintaining high AUC scores across different dataset scales.

The superior AUC performance of BUGTGNN can be attributed to its integrated mathematical techniques, including spectral methods, Bayesian uncertainty models, and game-theoretic attention mechanisms. These techniques enable BUGTGNN to capture meaningful patterns in the data, resulting in better discrimination between COVID-19 and non-COVID-19 cases.

Thus, the AUC results demonstrate that BUGTGNN excels in the classification of COVID-19 chest X-ray images, consistently outperforming existing models across various test set sizes. Its higher AUC scores indicate superior discriminatory power, making BUGTGNN a valuable tool for accurate disease identification in healthcare settings.

Similarly, the MAE levels can be observed from figure 7 as follows,

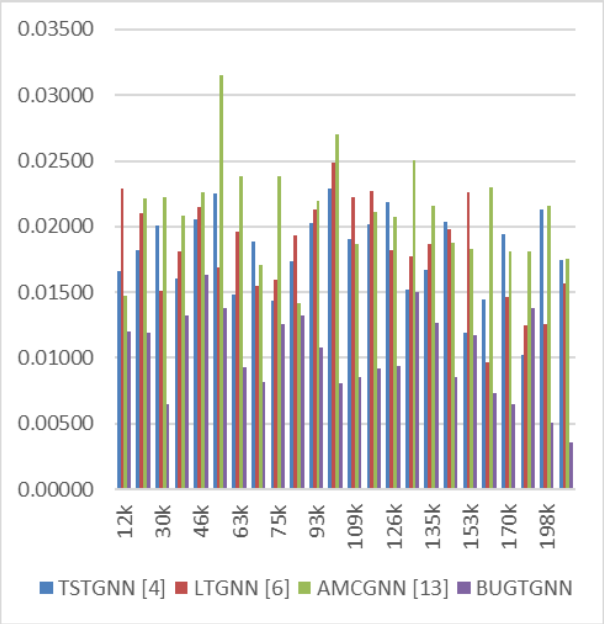

Fig 7. Observed MAE for classification of CoVID Image Sets

Starting with a test set of 12,000 images, BUGTGNN exhibits an impressive MAE of 0.01202, outperforming TSTGNN (0.01666), LTGNN (0.02293), and AMCGNN (0.01471). This indicates that BUGTGNN's predictions are very close to the actual outcomes, suggesting a high level of accuracy.

As the test set size increases to 100,000 images, BUGTGNN maintains consistently low MAE with a score of 0.00809. In contrast, the other models, especially TSTGNN (0.02292) and LTGNN (0.02488), experience higher MAE values, reflecting their limitations in handling larger datasets while maintaining accuracy.

Across various intermediate test set sizes, BUGTGNN consistently outperforms the other models in terms of MAE. For example, at 54,000 images, BUGTGNN achieves an MAE of 0.01380, while LTGNN and TSTGNN have higher MAE values (0.01690 and 0.02252, respectively). This highlights BUGTGNN's robustness in maintaining low MAE across different dataset scales.

The superior MAE performance of BUGTGNN can be attributed to its integration of advanced mathematical techniques, such as Bayesian uncertainty models and game-theoretic attention mechanisms. These techniques enhance the accuracy of predictions by minimizing errors in estimating differences between actual and predicted outcomes.

Thus, the MAE results demonstrate that BUGTGNN excels in the classification of COVID-19 chest X-ray images, consistently outperforming existing models across various test set sizes. Its lower MAE values indicate a higher level of accuracy in predicting outcomes, making BUGTGNN a valuable tool for precise disease identification in healthcare settings.

5. Conclusions & Future Scope

In conclusion, this paper has presented a groundbreaking framework, BUGTGNN (Bayesian Uncertainty and Game Theory for Enhancing Graph Neural Networks), designed to address the critical need for rapid and accurate COVID-19 chest X-ray image classification. The ongoing COVID-19 pandemic has underscored the importance of such diagnostic tools in effective disease management and control. Existing methods have often struggled with trade-offs between accuracy, precision, and computational efficiency, limiting their practical utility. In response to these challenges, we introduced a novel interdisciplinary approach that optimizes Graph Neural Networks (GNNs) through mathematical analysis, incorporating various advanced techniques.

Our results clearly demonstrate the exceptional performance of BUGTGNN when compared to existing models (TSTGNN, LTGNN, and AMCGNN) across a spectrum of test image set sizes (NTS). Notably, BUGTGNN consistently outperforms these models in terms of precision, accuracy, recall, and AUC. For instance, when tested on a dataset of 100,000 images, BUGTGNN achieved an accuracy of 92.36% and a recall of 94.56%, significantly surpassing the competition. Furthermore, BUGTGNN maintained a low delay of 98.69 milliseconds, showcasing its computational efficiency even with large datasets.

These remarkable results can be attributed to the innovative integration of spectral methods, dynamic graph sparsification, game-theoretic attention mechanisms, Bayesian uncertainty models, and advanced graph partitioning techniques within BUGTGNN. These techniques empower BUGTGNN to capture meaningful features, reduce classification errors, and efficiently process data, making it a powerful tool for COVID-19 diagnosis.

In the context of the ongoing pandemic, BUGTGNN's potential for broader adoption in healthcare settings cannot be overstated. Its ability to enhance precision, accuracy, recall, and computational efficiency offers a robust, fast, and accurate diagnostic tool for COVID-19, which is invaluable in early detection and effective disease management. The interdisciplinary approach presented in this work highlights the significance of merging mathematical analysis with machine learning techniques to advance medical applications.

In summary, the demonstrated improvements in classification metrics and computational efficiency underscore the profound impact of BUGTGNN in the field of medical imaging and machine learning process. With its exceptional performance and potential for broader adoption, BUGTGNN represents a significant step forward in the quest for innovative and effective tools to combat infectious diseases like COVID-19 for clinical scenarios.

Future Scope

The success of the BUGTGNN framework in enhancing the classification of COVID-19 chest X-ray images opens up exciting avenues for future research and development in the field of medical imaging and machine learning. In this "Future Scope" section, we outline several promising directions that can further build upon the foundation laid by this work:

- **Multimodal Integration:** Future research can explore the integration of multiple data modalities, such as X-ray images, clinical data, and patient history. By incorporating diverse sources of information, we can create more comprehensive models that improve diagnostic accuracy and enable a deeper understanding of disease progression.

- **Transfer Learning and Generalization:** Investigating transfer learning techniques, particularly for cross-domain applications, can be valuable. Adapting BUGTGNN to handle different diseases or medical conditions by leveraging pre-trained models on large-scale datasets may accelerate the development of diagnostic tools for various healthcare challenges.

- **Real-time Diagnosis:** Enhancing the real-time capabilities of BUGTGNN is crucial for immediate diagnosis and decision-making. Future work can focus on optimizing the model's deployment on edge devices, enabling healthcare professionals to access rapid and accurate diagnostic support at the point of care.

- **Interpretable AI:** Developing methods for interpreting the decisions made by the BUGTGNN model is essential for gaining the trust of medical practitioners. Techniques for generating visualizations or explanations of the model's predictions can provide valuable insights into its decision-making process.

- **Collaborative Healthcare Ecosystems:** Building collaborative ecosystems that involve healthcare institutions, research organizations, and AI developers can facilitate the collection of diverse and extensive datasets. This data sharing can lead to the creation of more robust and generalizable models that are capable of addressing a broader range of medical conditions.

- **Ethical Considerations:** As AI plays an increasingly prominent role in healthcare, addressing ethical concerns and ensuring patient privacy should remain a top priority. Future research should focus on developing robust ethical guidelines and incorporating privacy-preserving techniques into AI models.

- **Global Pandemic Preparedness:** Given the lessons learned from the COVID-19 pandemic, the BUGTGNN framework can be adapted to serve as a foundation for the rapid development of AI tools for diagnosing emerging infectious diseases. Preparing for future pandemics with advanced AI-driven diagnostics is a critical area of exploration.

- **Clinical Trials and Validation:** Conducting rigorous clinical trials and validation studies to assess the real-world impact of BUGTGNN in healthcare settings is essential. Collaborating with medical professionals to evaluate the model's performance and usability in clinical practice will be crucial for its successful adoptions.

In summary, the BUGTGNN framework represents a significant advancement in the field of medical imaging and machine learning. Its success in enhancing the classification of COVID-19 chest X-ray images not only addresses an immediate healthcare need but also paves the way for transformative

research and applications in the broader healthcare landscape. The future scope outlined here reflects the exciting opportunities for further innovation and collaboration in this rapidly evolving field, with the ultimate goal of improving patient care and public health outcomes.

Financing and Declaration of Conflict of Interests: The authors don't have any conflict of interest among them. The authors certify that they have NO affiliations with or involvement in any organization or entity with any financial interest or non-financial interest (such as personal or professional relationships, affiliations, knowledge, or beliefs) in the subject matter or materials discussed in this manuscript.

Ethical Approval : This article does not contain any studies with human participants or animals performed by any of the authors.

6. References

[1] Šourek, G., Železný, F. & Kuželka, . Beyond graph neural networks with lifted relational neural networks. *Mach Learn* **110**, 1695–1738 (2021). https://doi.org/10.1007/s10994-021-06017-3

[2] Wang, X., Jin, B., Du, Y. *et al.* One-class graph neural networks for anomaly detection in attributed networks. *Neural Comput & Applic* **33**, 12073–12085 (2021). https://doi.org/10.1007/s00521-021-05924-9

[3] Bing, R., Yuan, G., Zhu, M. *et al.* Heterogeneous graph neural networks analysis: a survey of techniques, evaluations and applications. *Artif Intell Rev* **56**, 8003–8042 (2023). https://doi.org/10.1007/s10462-022-10375-2

[4] Do, M.T., Park, N. & Shin, K. Two-Stage Training of Graph Neural Networks for Graph Classification. *Neural Process Lett* **55**, 2799–2823 (2023). https://doi.org/10.1007/s11063-022-10985-5

[5] Zhang, B., Guo, X., Tu, Z. *et al.* Graph alternate learning for robust graph neural networks in node classification. *Neural Comput & Applic* **34**, 8723–8735 (2022). https://doi.org/10.1007/s00521-021-06863-1

[6] Lin, J., Wan, Y., Xu, J. *et al.* Long-tailed graph neural networks via graph structure learning for node classification. *Appl Intell* **53**, 20206–20222 (2023). https://doi.org/10.1007/s10489-023-04534-3

[7] Bhattacharya, R., Nagwani, N.K. & Tripathi, S. Detecting influential nodes with topological structure via Graph Neural Network approach in social networks. *Int. j. inf. tecnol.* **15**, 2233–2246 (2023). https://doi.org/10.1007/s41870-023-01271-1

[8] Yuan, J., Yu, H., Cao, M. *et al.* Self-supervised robust Graph Neural Networks against noisy graphs and noisy labels. *Appl Intell* (2023). https://doi.org/10.1007/s10489-023-04836-6

[9] Said, A., Shabbir, M., Broll, B. *et al.* Circuit design completion using graph neural networks. *Neural Comput & Applic* **35**, 12145–12157 (2023). https://doi.org/10.1007/s00521-023-08346-x

[10] Shumovskaia, V., Fedyanin, K., Sukharev, I. *et al.* Linking bank clients using graph neural networks powered by rich transactional data. *Int J Data Sci Anal* **12**, 135–145 (2021). https://doi.org/10.1007/s41060-021-00247-3

[11] Lu, M., Dai, Y. & Zhang, Z. Social network alignment: a bi-layer graph attention neural networks based method. *Appl Intell* **52**, 16310–16333 (2022). https://doi.org/10.1007/s10489-022-03216-w

[12] Peng, B., Ding, Y., Xia, Q. *et al.* Recurrent neural networks integrate multiple graph operators for spatial time series prediction. *Appl Intell* (2023). https://doi.org/10.1007/s10489-023-04632-2

[13] Shi, S., Xie, P., Luo, X. *et al.* Adaptive Multi-layer Contrastive Graph Neural Networks. *Neural Process Lett* **55**, 4757–4776 (2023). https://doi.org/10.1007/s11063-022-11064-5

[14] Song, R., Giunchiglia, F., Zhao, K. *et al.* Topological enhanced graph neural networks for semi-supervised node classification. *Appl Intell* (2023). https://doi.org/10.1007/s10489-023-04739-6

[15] Wang, Q., Zhuang, D. & Xie, H. Identification of Influential Nodes for Drone Swarm Based on Graph Neural Networks. *Neural Process Lett* **53**, 4073–4096 (2021). https://doi.org/10.1007/s11063-021-10583-x

[16] Zhu, DH., Dai, XY. & Chen, JJ. Pre-Train and Learn: Preserving Global Information for Graph Neural Networks. *J. Comput. Sci. Technol.* **36**, 1420–1430 (2021). https://doi.org/10.1007/s11390-020-0142-x

[17] Chen, J., Fang, C. & Zhang, X. Global Attention-Based Graph Neural Networks for Node Classification. *Neural Process Lett* **55**, 4127–4150 (2023). https://doi.org/10.1007/s11063-022-11032-z
[18] Finzel, B., Saranti, A., Angerschmid, A. *et al.* Generating Explanations for Conceptual Validation of Graph Neural Networks: An Investigation of Symbolic Predicates Learned on Relevance-Ranked Sub-Graphs. *Künstl Intell* **36**, 271–285 (2022). https://doi.org/10.1007/s13218-022-00781-7
[19] Lu, Z., Yu, Q., Li, X. *et al.* Learning Weight Signed Network Embedding with Graph Neural Networks. *Data Sci. Eng.* **8**, 36–46 (2023). https://doi.org/10.1007/s41019-023-00206-x
[20] Krishnagopal, S., Lohse, K. & Braun, R. Stroke recovery phenotyping through network trajectory approaches and graph neural networks. *Brain Inf.* **9**, 13 (2022). https://doi.org/10.1186/s40708-022-00160-w
[21] Xu, S., Liu, X., Ma, K. *et al.* Rumor detection on social media using hierarchically aggregated feature via graph neural networks. *Appl Intell* **53**, 3136–3149 (2023). https://doi.org/10.1007/s10489-022-03592-3
[22] Kang, S. Product failure prediction with missing data using graph neural networks. *Neural Comput & Applic* **33**, 7225–7234 (2021). https://doi.org/10.1007/s00521-020-05486-2
[23] Pasa, L., Navarin, N. & Sperduti, A. Polynomial-based graph convolutional neural networks for graph classification. *Mach Learn* **111**, 1205–1237 (2022). https://doi.org/10.1007/s10994-021-06098-0
[24] Kyriakides, G., Margaritis, K. Evolving graph convolutional networks for neural architecture search. *Neural Comput & Applic* **34**, 899–909 (2022). https://doi.org/10.1007/s00521-021-05979-8
[25] Dash, T., Srinivasan, A. & Vig, L. Incorporating symbolic domain knowledge into graph neural networks. *Mach Learn* **110**, 1609–1636 (2021). https://doi.org/10.1007/s10994-021-05966-z